HPV16 E6/E7 promote the translocation and glucose uptake of GLUT1 by PI3K/AKT pathway *via* relieving miR-451 inhibitory effect on CAB39 in lung cancer cells

Hong-Miao Wang, Ying-Jie Lu, Ling He, Na-Jin Gu, Shi-Yu Wang, Xue-Shan Qiu, En-Hua Wang and Guang-Ping Wu iD

Abstract

Background: HPV16 E6/E7 proteins are the main oncogenes and only long-term persistent infection causes lung cancer. Our previous studies have shown that HPV16 E6/E7 protein up-regulates the expression of GLUT1 in lung cancer cells. However, whether E6 and E7 protein can promote the glucose uptake of GLUT1 and its molecular mechanism are unclear.

Methods: The regulatory relationships of E6 or E7, miR-451, CAB39, PI3K/AKT, and GLUT1 were detected by double directional genetic manipulations in lung cancer cell lines. Immunofluorescence and flow cytometry were used to detect the effect of CAB39 on promoting the translocation to the plasma membrane of GLUT1. Flow cytometry and confocal microscopy were performed to detect the glucose uptake levels of GLUT1.

Results: The overexpression both E6 and E7 proteins significantly down-regulated the expression level of miR-451, and the loss of miR-451 further up-regulated the expression of its target gene CAB39 at both protein and mRNA levels. Subsequently, CAB39 up-regulated the expression of GLUT1 at both protein and mRNA levels. Our results demonstrated that HPV16 E6/E7 up-regulated the expression and activation of GLUT1 through the HPV–miR-451–CAB39–GLUT1 axis. More interestingly, we found that CAB39 prompted GLUT1 translocation to the plasma membrane and glucose uptake, and this promotion depended on the PI3K/AKT pathway.

Conclusion: Our findings provide new evidence to support the critical roles of miR-451 and CAB39 in the pathogenesis of HPV-related lung cancer.

Keywords: CAB39, GLUT1, HPV16, lung cancer, miR-451, PI3K/AKT

Received: 5 May 2020; revised manuscript accepted: 18 August 2020.

Correspondence to:
Guang-Ping Wu
Department of Pathology,
The First Affiliated
Hospital and College of
Basic Medical Sciences,
China Medical University,
No. 155 Nanjing Bei Street,
Heping District, Shenyang
110001, China
wug_ping@sina.com

Hong-Miao Wang
Ling He
Na-Jin Gu
Xue-Shan Qiu
En-Hua Wang
Department of Pathology,
The First Affiliated
Hospital and College of
Basic Medical Sciences,
China Medical University,
Shenyang, China

Ying-Jie Lu
Department of
Dermatology, Jilin
Province People's
Hospital, Changchun,
China

Shi-Yu Wang
Department of Internal
Medicine, White River
Health System, Batesville,
AR, USA

Introduction

As a tumor suppressor gene, miR-451 is aberrantly expressed in many cancer cells, such as in glioma,[1] cutaneous basal cell carcinoma,[2] hepatoma,[3] colorectal carcinoma,[4] and in lung cancer cells.[5] It plays an important role in cancer development and metastasis.[6] The loss of miR-451 initiates and accelerates the proliferation and migration of cancer cells and predicted worse prognosis in non-small cell lung cancer (NSCLC) cases.[7] Liu *et al.* reported that miR-451 inhibited the proliferation and migration of NSCLC cells *via* LKB1/AMPK pathways.[5] Several other studies have shown that miR-451 inhibits the growth of cancer cells *via* down-regulated phosphatidylinositol-3 kinase (PI3K)/AKT signaling pathway by directly inhibiting its target gene calcium-binding protein 39 (CAB39).[4,8,9] CAB39 is a key regulator of a group of sterile 20 kinases, and Jiang *et al.* reported that CAB39 promoted hepatocellular carcinoma growth and metastasis.[10] Gou *et al.* demonstrated that miR-451 negatively regulated GLUT1 by targeting CAB39 in glioma cells.[1]

It is well known that the cancer cells use the Warburg effect to consume more glucose to obtain energy by aerobic glycolysis. During this process, activated GLUT1, the main glucose transporter, plays a critical role. GLUT1 is up-regulated on a variety of tumor cell plasma membranes, including lung cancer cells.[11] The key role that GLUT1 plays in the Warburg effect is not to increase the expression of GLUT1 in the cytoplasm, but to be activated. Mechanism studies have shown that the activation of GLUT1 is mainly through stimulating to increase the translocation of GLUT1 from the cytoplasm to the plasma membrane, thus promoting the glucose uptake of GLUT1.[12,13]

Since Syrjänen first hypothesized that human papillomavirus (HPV) infection might play an important role in the occurrence of lung cancer[14] in 1979, an increasing number of studies have shown that HPV16 E6/E7 proteins were the main oncogenes,[15] and only long-term persistent infection could cause lung cancer.[16] Our previous studies demonstrated that HPV16 E6/E7 proteins up-regulated GLUT1 at both protein and mRNA levels in four well-established lung cancer cell lines.[17,18]

Thus, the investigation of the relationship among HPV16 E6/E7, miR-451, and GLUT1 is our main aim in the current study. Using double directional genetic manipulations in the well-established lung cancer cell lines, we show that both E6 and E7 proteins significantly down-regulate the expression level of miR-451, and the loss of miR-451 further up-regulates the expression of its target gene, calcium binding protein 39 (CAB39), at both the protein and mRNA levels. Subsequently, CAB39 up-regulates the expression of GLUT1 at both protein and mRNA levels. Our results demonstrate that HPV16 E6/E7 proteins up-regulate the expression of GLUT1 through the HPV–miR-451–CAB39–GLUT1 axis. More interestingly, we found that CAB39 prompted GLUT1 translocation to the plasma membrane and glucose uptake. We further confirmed that CAB39 promoted GLUT1 through PI3K/AKT pathways.

Materials and methods

The study was conducted according to the guidelines of the institutional review boards at the First Affiliated Hospital of China Medical University; we had obtained an internal review board approval for this study.

Cell culture

Three human non-small cell lung carcinoma (NSCLC) cell lines H460, A549, LK2, and the normal human bronchial epithelial (HBE) cell line were used in this study. HBE was used as a control to determine the expression levels of miR-451 and CAB39.[19] HBE, H460, and A549 cell lines were purchased from the cell bank of Chinese Academy of Science (Shanghai, China). HBE was cultured in Hyclone (Logan, UT, USA) minimum Eagle's medium (MEM) supplemented with 10% fetal bovine serum (FBS; Cellmax, Beijing, China). H460 and A549 were cultured in Hyclone RPMI 1640 medium supplemented with 10% FBS. The LK2 cell line was obtained from Dr. Hiroshi Kijima (Department of Pathology and Bioscience, Hirosaki University Graduate School of Medicine, Japan) and cultured in Hyclone Dulbecco's modified Eagle's medium (DMEM) supplemented with 10% FBS. Cells were cultured in a humidified incubator at 37°C with 5% CO_2.

Plasmid construction and small-interfering RNA

The plasmids for pEGFP-N1-HPV16 E6, pEGFP-N1-HPV16 E7, and pEGFP-N1 were kindly provided by Professor Xudong Tang (Institute of Biochemistry and Molecular Biology, Guangdong Medical College, China). The mimics for mirRNA-451-on or mirRNA-mimic were purchased from GenePharma (Shanghai, China). The plasmids pCMV3-C-Myc-CAB39 and pCMV3-C-Myc were purchased from Sino Biological (Sino Biological, Inc., USA). Small-interfering RNA (siRNA) was performed to silence the expression of specific genes. The siRNAs against HPV16 E6 and HPV16 E7 were purchased from RIBOBIO (Guangzhou, China) and the scrambled siRNA (sc-37007) were purchased from Santa Cruz Biotechnology (Santa Cruz, CA, USA) as a nonspecific siRNA control. The CAB39 siRNA and scrambled siRNA were purchased from RIBOBIO (Guangzhou, China).

To inhibit PI3K/AKT signaling, cells were treated with 10 μM Miltefosine (ApexBio, USA), an inhibitor that blocks the PI3K/AKT pathway. Miltefosine was dissolved in dimethyl sulfoxide

Table 1. Sequences and features of primers used for qRT-PCR.

Gene	Forward Reverse	Sequence (5'–3')	Size (bp)	Melting (°C)	mRNA
E6	270	GTATGGAACAACATTAGAACAGCAA	79	54.65	KX545363
	349	GTGGCTTTTGACAGTTAATACACC		53.55	
E7	482	GCATGGAGATACACCTACATTG	273	51	KX545363
	754	TGGTTTCTGAGAACAGATGG		58	
CAB39	1211	TGAACCTGCTGCGAGACAAAA	88	60	NM_016289.4
	1298	TGCGTCTTGTTAGGATTGGCTA		60	
GLUT1	1071	CTGGCATCAACGCTGTCTTC	167	60	NM_006516.3
	1237	GCCTATGAGGTGCAGGGTC		60	
GAPDH	50	TTCTTTTGCGTCGCCAGCCGAG	71	51.06	XM_019023188.1
	120	CCAGGCGCCCAATACGACCAAA		51.06	
miR-451		CCTCGCAAACCGTTACCATT		62	
		TATCCTTGTTCACGACTCCTTCAC		62	
U6		CGCTTCGGCAGCACATATAC		62	
		TTCACGAATTTGCGTGTCATC		62	

mRNA, messenger RNA; miR, micro RNA; qRT-PCR, quantitative real-time reverse transcriptase polymerase chain reaction.

(DMSO) and added 12 h after a 36-h transfection, with the same volume of DMSO added to control cells.

Transfection and interference

The transfection and interference have been described previously.[16]

Quantitative real-time PCR assays

Total RNA was extracted from cells using RNAiso Plus (TaKaRa, Japan) according to the manufacturer's instructions. Total 600 ng RNA was subjected to reverse transcription reaction to obtain cDNAs by using the Prime Script TM RT reagent Kit (TaKaRa, Japan) as follow: 37°C for 15 min, 85°C for 5 s, and the quantitative real-time reverse transcriptase polymerase chain reaction (qRT-PCR) was performed on 7900HT Fast Real-Time PCR System (Applied Biosystems) using SYBR® Premix Ex Taq II (TaKaRa, Japan) as follows: 95°C for 2 min, 40 cycles of 95°C for 15 s, 60°C for 60 s. A total of 3000 ng RNA miR-451 and U6 were subjected to reverse transcription reaction to obtain cDNAs by using the Hairpin-itTM miRNAs qPCR Quantitation Kit (GenePharma, China) as follows: 25°C for 30 min, 42°C for 30 min, 85°C for 5 min. The qRT-PCR was performed using the Hairpin-itTM miRNAs qPCR Quantitation Kit as follows: 95°C for 3 min, 40 cycles of 95°C for 12 s, 62°C for 40 s. A dissociation procedure was performed to generate a melting curve for confirmation of amplification specificity. GAPDH and U6 were used as the reference gene. The relative levels of gene expression were represented as $\Delta Ct = Ct$ gene – Ct reference, and the fold change of gene expression was calculated by the $2^{-\Delta\Delta Ct}$ method. Experiments were repeated in triplicate. The detailed information of the primers is given in Table 1.

Western blot analysis

Western blot analysis was performed to quantify the amount of target protein. The Western blot has been described previously.[16] HPV16 E6 (1:700, Abcam, Boston, MA, USA), HPV16 E7 (1:200, Bioss, Beijing, China), CAB39 (1:1000; Cell Signaling Technology, Beverly, MA, USA), PI3K(P85α) (1:1000; Proteintech, Wuhan, China), P-AKT(ser473) (1:1000; Proteintech), AKT (1:1000; Proteintech), GLUT1 (1:500; Wanleibio, China), and GAPDH (1:15000, Proteintech). After the membranes were further incubated with appropriate horseradish peroxidase (HRP)-conjugated anti-mouse or anti-rabbit IgG (1:5000; Proteintech) at 37°C for 2 h, the immunosignal was detected by using ECL Western blot kit (advansta, USA). The bands were analyzed with BioImaging systems (UVP Inc., Upland, CA, USA).

Immunofluorescence

Cells with 90% confluent were seeded into a six-well culture plate. After gene transfection or siRNA interference was performed, the cells were cultured for another 24 h. Then the cells with a concentration of 5×10^4 cell/ml (500 μl/well of the cell suspension) were seeded into a 24-well culture plate. Each bottom of the 24 wells were pre-inserted a 15 mm round cover glass slide (NEST Biotechnology Co., China) and the cells were cultured for 24 h to form a confluent monolayer. The cells were washed with ice-cold PBS and fixed with 4% formaldehyde (Solarbio, Beijing, China) for about 20 min. After the permeability treatment with PBS containing 0.1% Triton X-100 (Solarbio, Beijing, China) for 15 min and blocked with 3% bovine serum albumin for 1 h at 37°C. Subsequently, the coverslips were incubated with CAB39 (1:50; Cell Signaling, USA) or GLUT1 (1:50; Proteintech) antibody at 4°C overnight. After incubation with CoraLite488-conjugated Affinipure Goat Anti-Rabbit IgG (H+L) secondary antibody (SA00013-2, PTG, Beijing, China) for 1 h, the cover slips were mounted in Prolong Gold antifade reagent with DAPI (Beyotime, Shanghai, China) for 5 min, and coverslipped. Images were obtained on a confocal microscope (Carl Zeiss, Germany)

Glucose uptake assay

Cells (2–5×10^4 cells/well) were seeded 1 day before starting the assay. After 12 h, regular culture medium (10% FBS) were removed and cells were treated with CAB39 transfected or untransfected in 400 μl cell culture medium with 0.5% FBS and incubated at 37°C with 5% CO_2 for 3 h. Then 4 μl of fluorescent glucose analog 2-NBDG (2-N-[(7-nitrobenz-2-oxa-1,3-diazol-4-yl) amino]-D-glucose; BioVision, CA, USA) was added to each sample and incubated at 37°C with 5% CO_2 for 30 min. After incubation, the cells from the plate were kept on ice and washed once with 1 ml ice-cold 1X Analysis Buffer. Two methods were adopted for measuring the levels of glucose uptake. One analysis was performed using flow cytometry. Briefly, the cells were collected from the plates and the cell pellet was resuspended in 400 μl of 1X Analysis Buffer and analyzed on a flow cytometer (488 nm excitation laser; BD Accuri™ C6 Plus personal flow cytometer, USA). For flow acquisition and analysis mounting, the main cell groups were selected in the Forward scatter (FSC) *versus* Side scatter (SSC) plot to exclude dead cells and cellular debris. Within the main cell population, mean fluorescence intensity in FL1 was quantified and compared between cells treated with CAB39 transfected and untreated control cells. The other analysis was performed by using confocal microscopy to perform the image analysis. Briefly, the cells seeded into a 24-well culture plate were washed with 200 μl of fresh 1X Analysis Buffer and the images were acquired immediately under a confocal microscope using a blue excitation fluorescence filter (excitation range 420–495 nm). The fluorescence intensity was kept at a minimum to minimize photo-bleaching. Images were taken randomly from at least five different fields.

Statistical analysis

SPSS 22.0 software was utilized for statistical analyses in this study. Each assay was performed at least three times. The data were expressed as mean ± SD and the significance of differences in multiple comparisons was determined by Student's *t*-test. $p < 0.05$ was considered to be statistically significant.

Results

The screening of lung cancer cell lines

Based on our previous results, H460 cells were low E6 and E7 expression cell lines, and A549 and LK2 cells were high E6 and E7 expression

cell lines.[17] To investigate the roles of miR-451 and CAB39 on regulating GLUT1 translocation to the plasma membrane in lung cancer cell, several lung cancer cell lines were tested and three cell lines, A549, LK2, and H460, were selected. The HBE cell line was selected to be used as a control for the expression levels of miR-451 and CAB39: higher than HBE was considered as high expression and lower than HBE was considered as low expression. The expression level of miR-451 was high in LK2, but low in A549 and H460 (Supplemental Figure A). The expression level of CAB39 was high in A549, medium in LK2, and low in H460 (Supplemental Figure B). Low expression level of GLUT1 on the plasma membrane was observed in all three cell lines (Supplemental Figure C). Low glucose uptake (average fluorescence intensity per cell) happened in all three cell lines (Supplemental Figure D). Further assays were designed and performed based on these results.

HPV16 E6/E7 down-regulated the expression of miR-451 but up-regulated the expression of CAB39, PI3K (P85α), P-AKT (ser473), and GLUT1

The pEGFP-N1-E6 or E7 vectors were transiently transfected into the low expression H460 cell line. Overexpression of E6 or E7 significantly down-regulated the expression of miR-451, but up-regulated the expression of CAB39, PI3K (P85α), and P-AKT (ser473) at protein levels only, as well as up-regulated the expression of GLUT1 at both protein and mRNA levels. The expression of AKT showed minimal or no change. The results are presented in Figure 1A. On the other hand, the inhibition of both E6 and E7 received the opposite results in A549 and LK2 cells, and they are presented in Figure 1B and C.

miR-451 down-regulated the expression of CAB39, PI3K (P85α), P-AKT (ser473), and GLUT1

The Hsa-miR-451 was transiently transfected into the low expression H460 and A549 cell lines. The overexpression of miR-451 significantly down-regulated the expression of CAB39 and GLUT1 at both protein and mRNA levels, and the expression of PI3K (P85α) and P-AKT (ser473) at the protein level only. The expression of AKT showed minimal or no change. The results were presented in Figure 2A and B. The converse results were achieved when we inhibited the expression of miR-451 in the high expression LK2 cells and the results were presented in Figure 2C.

CAB39 up-regulated the expression of PI3K (P85α), P-AKT (ser473), and GLUT1

The pCMV3-C-Myc-CAB39 vector was transiently transfected into the H460 and LK2 cell lines. The results showed that overexpression of CAB39 significantly up-regulated the expression of GLUT1 at both protein and mRNA levels, and the expression of PI3K (P85α) and P-AKT (ser473) at the protein level only whereas the expression of AKT showed minimal or no change (Figure 3A and B). The opposite results of inhibitory effect of CAB39 in A549 and LK2 cells were presented in Figure 3C and D.

CAB39 promoted the activation of GLUT1 and the promotion was dependent on the PI3K/AKT pathway

The overexpression of CAB39 significantly promoted both the plasma membrane translocation and the glucose uptake of GLUT1 in the H460 and LK2 cells, the results are presented in Figure 4.

The image analysis data showed that GLUT1 expression could only be detected on the plasma membrane transfected with CAB39, but not on the plasma membrane transfected with empty vectors. Compared with the plasma membrane transfected with empty vector, the percentages of GLUT1 expression on the plasma membrane of transfected CAB39 were significantly higher in H460 (45.5%) and LK2 (67.1%) cells. The results are presented in Figure 4A and B.

The flow cytometry data showed that the glucose mean density was 4.3 times higher in H460 cells transfected with CAB39 than that transfected with empty vectors ($p \leq 0.01$), and 3.0 times higher in LK2 cells transfected with CAB39 than that transfected with empty vectors ($p \leq 0.01$), the results are presented in Figure 4C and the image by confocal microscope analysis are presented in Figure 4D.

To further verify whether the promotion of CAB39 was dependent on the PI3K/ATK pathway, we used a specific PI3K/AKT blocker, Miltefosine, to inhibit the PI3K/AKT pathway
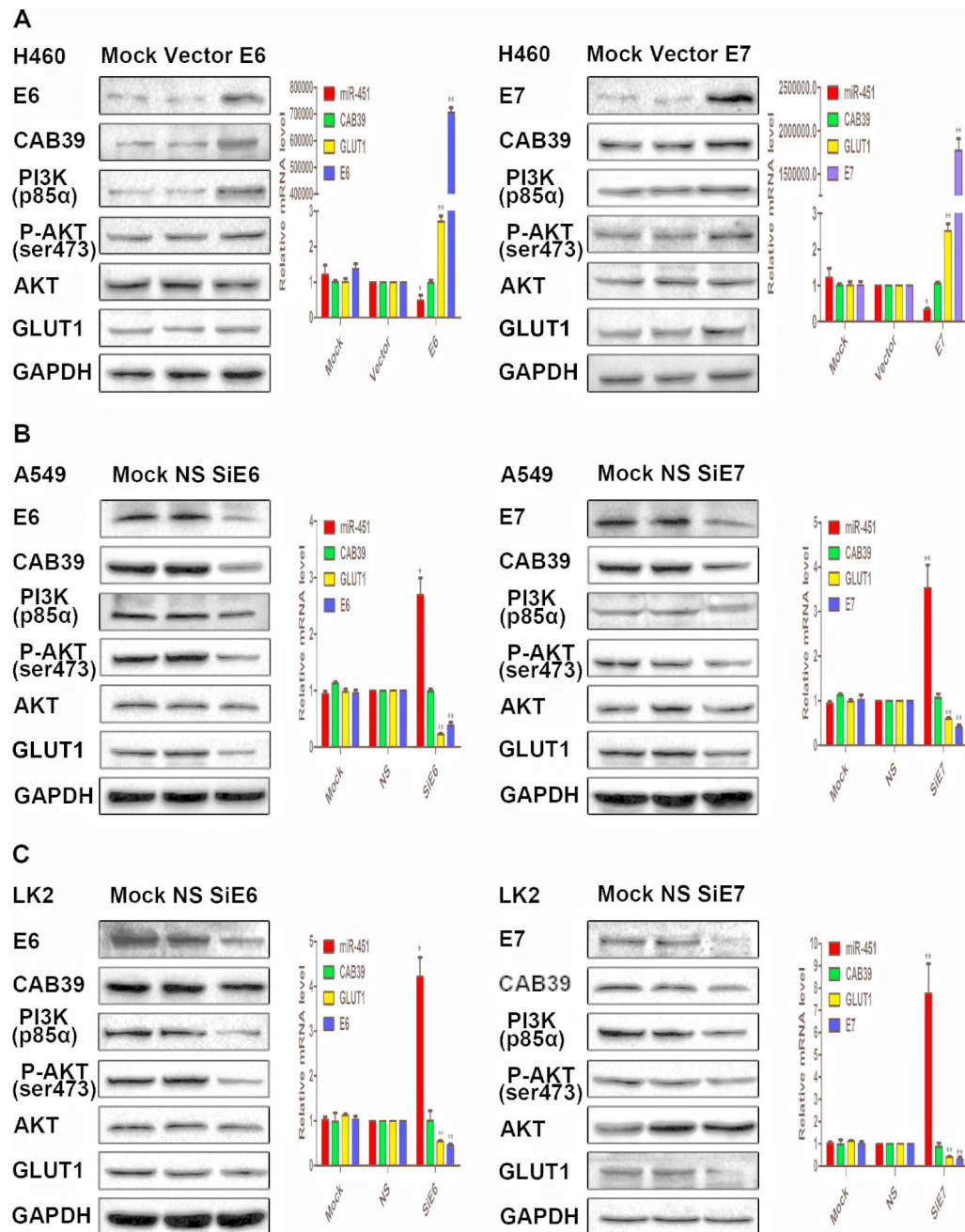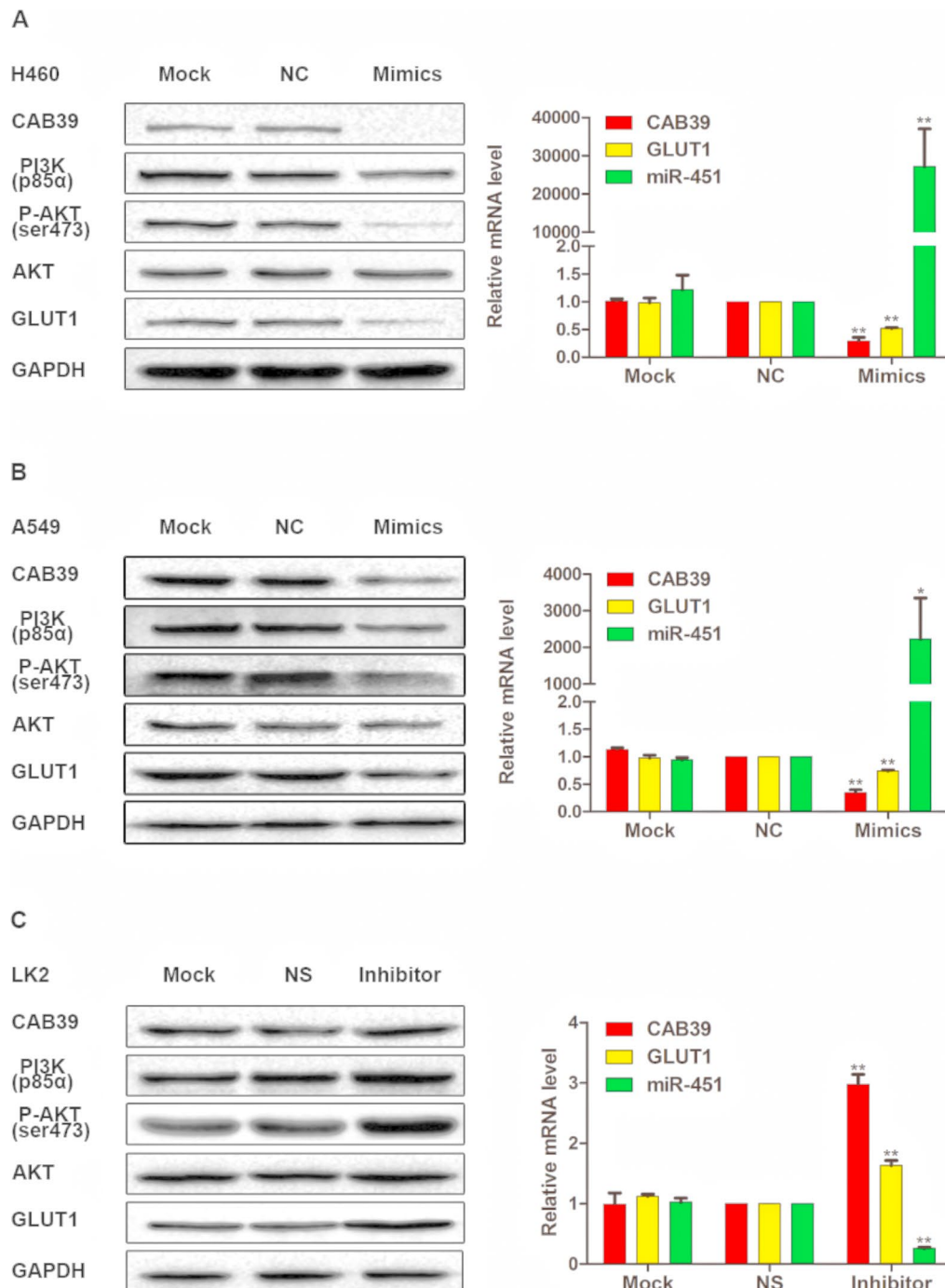
Figure 1. HPV16 E6/E7 down-regulated the expression of miR-451 but up-regulated the expression of CAB39, PI3K (P85α), P-AKT (ser473), and GLUT1. Proteins of E6, E7, CAB39, PI3K (P85α), P-AKT (ser473), AKT, and GLUT1 were demonstrated by Western blotting and the mRNAs of E6, E7, miR-451, CAB39, and GLUT1 were demonstrated by qRT-PCR in H460 or A549 or LK2 cells.
Mock, mock transfection or mock siRNA; NS, nonspecific siRNA; Vector, empty vector; qRT-PCR, quantitative real-time reverse transcriptase polymerase chain reaction.
$^*p < 0.05$; $^{**}p < 0.0l$.

in CAB39 transfected H460 and LK2 cell lines. The results showed that the promotion effects of CAB39 on GLUT1 protein expression, plasma membrane translocation, and glucose uptake were reversed. The results are presented in Figure 5.
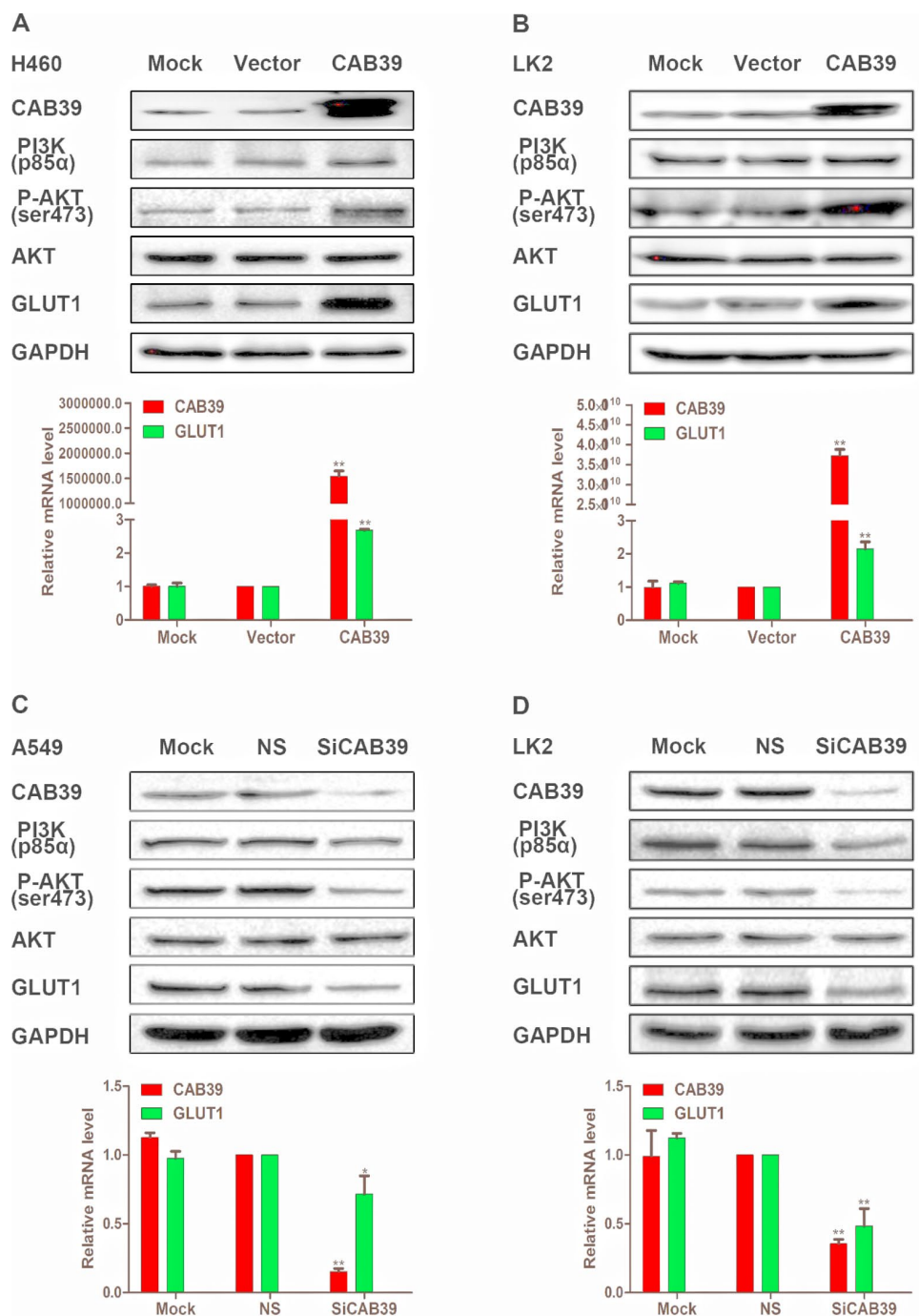
Figure 2. miR-451 down-regulated the expression of CAB39, PI3K (P85α), P-AKT (ser473), and GLUT1. Proteins of CAB39, PI3K (P85α), P-AKT (ser473), AKT, and GLUT1 were demonstrated by Western blotting and the mRNAs of miR-451, CAB39, and GLUT1 were demonstrated by qRT-PCR in H460 or A549 or LK2 cells. Mock, mock transfection or mock siRNA; NC, negative control; NS, nonspecific siRNA; Mimics, Hsa-miR-451 mimics; Inhibitor, miR-451 inhibitor; qRT-PCR, quantitative real-time reverse transcriptase polymerase chain reaction. $^*p < 0.05$; $^{**}p < 0.0$l.

Discussion

In our previous studies, we found that HPV16 E6/E7 proteins up-regulated the expression of GLUT1 at protein and mRNA levels,[17] but whether they promoted the membrane localization and the glucose uptake of GLUT1 was

Figure 3. CAB39 up-regulated the expression of PI3K (P85α), P-AKT (ser473), and GLUT1. Proteins of CAB39, PI3K (P85α), P-AKT (ser473), AKT, and GLUT1 were demonstrated by Western blotting and the mRNAs of CAB39 and GLUT1 were demonstrated by qRT-PCR in H460 or A549 or LK2 cells.
Mock, mock transfection or mock siRNA; NS, nonspecific siRNA; Vector, empty vector; ; qRT-PCR, quantitative real-time reverse transcriptase polymerase chain reaction.
$^*p < 0.05$; $^{**}p < 0.0l$).

unclear. Both the membrane localization and the glucose uptake of GLUT1 play important roles in the Warburg effect.[20] In this study, we have provided evidence that the overexpression of both E6 and E7 in HPV16 down-regulated the expression level of miR-451 in lung cancer cells.
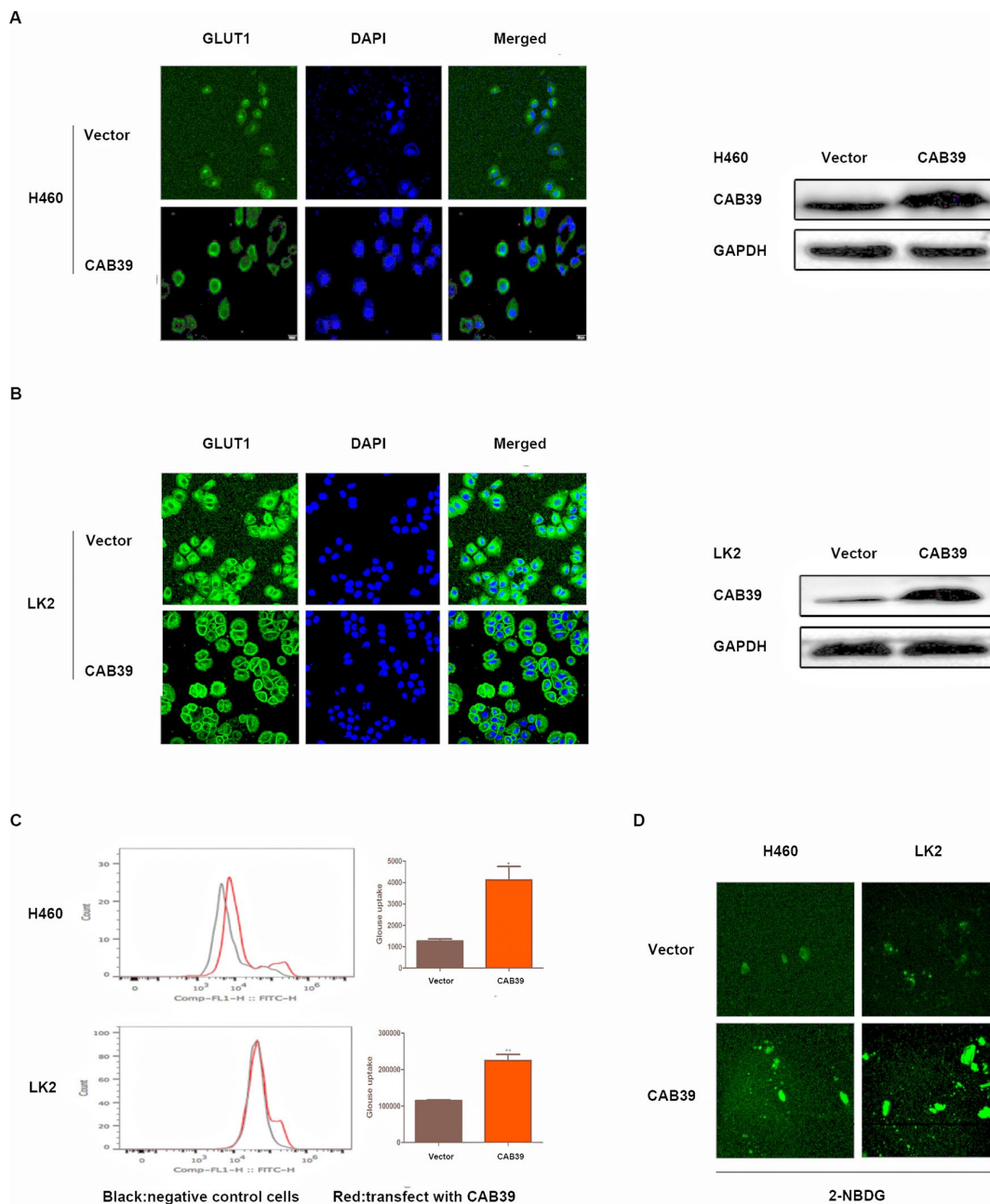
Figure 4. The image analysis results showed that the expression of GLUT1 on membrane was detected in cells transfected with cab39. Compared with un-transfected cells, the expression rates of GLUT1 in H460 cells (A) and LK2 cells (B) were 45.5% and 67.1%, respectively. Efficiency was measured by Western blotting. (C) The results of flow cytometry showed that the average density of glucose in H460 cells transfected with cab39 increased by 3.3 times ($p < 0.01$), and that in LK2 cells transfected with cab39 increased by 2.0 times ($p < 0.01$). (D) After 30 min of culture with fluorescent glucose analog 2-NBDG, clear images were obtained by confocal microscopy.
Vector, empty vector.

However, because the carcinogenesis mechanism of E6 and E7 proteins is not the same, the regulation pathways of miR-451 by both proteins may not be the same. The detailed differences need to be further studied in the future. The knockdown of miR-451 up-regulated the expression of
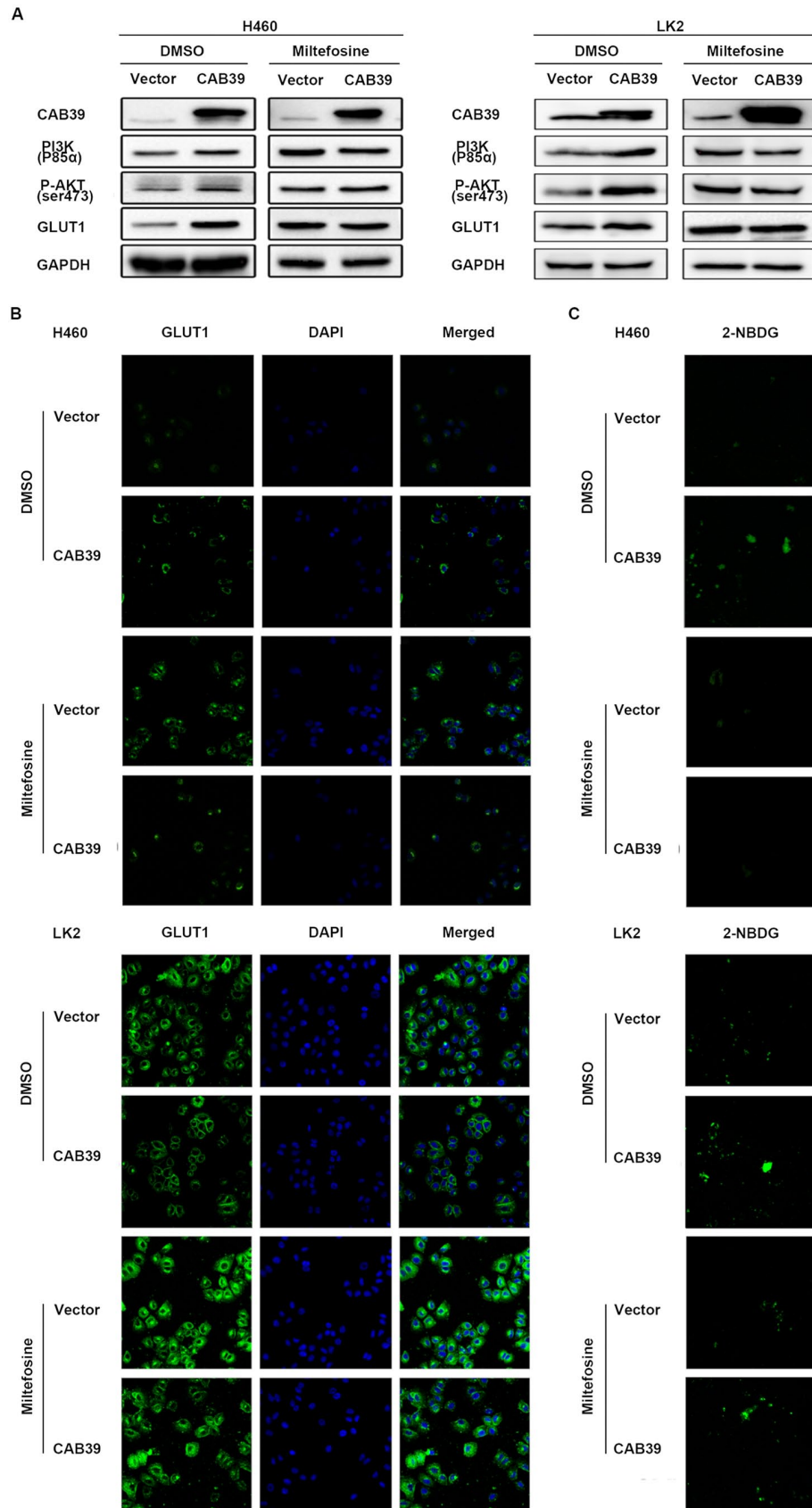
Figure 5. *(Continued)*

Figure 5. CAB39 promoted the activation of GLUT1 and the promotion was dependent on the PI3K/AKT pathway. (A) A specific PI3K/AKT blocker, Miltefosine, inhibited the PI3K/AKT pathway in both H460 and LK2 cell lines transfected with cab39, the results showed that the effects of CAB39 on the expression of GLUT1 protein were reversed. (B) The results of image analysis showed that the promoting effects of CAB39 on GLUT1 translocation to the plasma membrane were reversed by confocal microscopy. (C) The promoting effects of CAB39 on the glucose uptake of GLUT1 were reversed by confocal microscopy. Vector, empty vector.

CAB39 at both protein and mRNA levels, subsequently CAB39 up-regulated the expression of GLUT1 at both protein and mRNA levels. The overexpression of CAB39 also promoted the membrane translocation and the glucose uptake of GLUT1. Thus, we demonstrated that miR-451 acted as a safeguard against HPV-stimulated aerobic glycolysis and tumorigenesis by inhibiting its two down-stream effectors CAB39 and GLUT1. Our results provide new molecular mechanisms in HPV16 E6/E7 that promote both the membrane translocation and the glucose uptake of GLUT1 by relieving miR-451 inhibitory effect on CAB39 in lung cancer cells.

The expression level of miR-451 was low in NSCLC tissues by miRNA chips,[21] and the expression levels was related with tumor differentiation, pathologic stage, and lymph node metastasis.[4] The overexpression of miR-451 significantly inhibited both the proliferation and the migration of NSCLC cells *in vitro*.[7] Our conclusion was consistent with previous *in vitro* studies.

It is well known that the cancer cells consume more glucose to obtain energy by the Warburg effect.[22] The activated GLUT1 on the plasma membrane of tumor cells transports a large amount of glucose from the outside of cells to the mitochondria to provide the energy. However, the activation of GLUT1 is not related directly to the expression level of GLUT1 in cytoplasm, because most of the overexpressed GLUT1 in the cytoplasm are in a nonfunctional state, which are not able to play the role of the "Porter" of glucose.[23] The activation of GLUT1 depends first on its translocation from the cytoplasm to the plasma membrane, and second on its glucose uptake.[12,13] Barnes *et al.* showed that the mechanisms involved in regulating GLUT1 activation were associated with stimulation of AMP-activated protein kinase (AMPK) activity.[24] Egert et al. showed that GLUT1 translocation to the plasma membrane might be triggered by insulin in a phosphoinositide 3-kinase (PI3K)-dependent fashion.[25] Lee *et al.* demonstrated that protein kinase C involved in

phosphorylation of GLUT1 can lead to a rapid increase in glucose uptake and enhanced cell surface localization of GLUT1 induced by 12-0-tetra-decanoyl-phorbol-13-acetate (TPA).[26] Two studies showed that the expression of GLUT1 on plasma membrane in ovarian cancer cells was related to the activation of AKT.[27,28] Other studies indicated that LKB1 inhibited AKT activity in prostate cancer and melanoma cells.[29,30] Very recently, Liemburg-Apers *et al.* showed that GLUT1 activation was mediated by LKB1-dependent AMPK activation. Knockdown LKB1 activated AMPK to phosphorylated Sirt2, which further lead to the activation of mTOR–RAPTOR and of GLUT1 through an unknown but possible AKT-independent mechanism.[31]

Based on this evidence, we further explored the regulatory effect of CAB39 on the activation of GLUT1. We found that the transfection of CAB39 prompted GLUT1 translocation to the plasma membrane. To further confirm whether CAB39 promoted GLUT1 plasma membrane translocation was dependent on the PI3K/AKT pathway, we used a specific inhibitor, Miltefosine,[32] to inhibit the PI3K/AKT pathway in the cells transfected with CAB39 and the results showed that the effects of CAB39 on the GLUT1 protein expression, plasma membrane translocation, and glucose uptake were reversed. Our results demonstrate for the first time that the activation of CAB39 was one of the key steps for GLUT1 translocation to the plasma membrane and glucose uptake.

In conclusion, we have demonstrated that HPV16 E6/E7 proteins inhibited the expression of miR-451 in lung cancer cells, the down-regulation of miR-451 further up-regulated the expression of CAB39, and subsequently up-regulated GLUT1. Our results proposed an HPV–miR-451–CAB39–GLUT1 axis for the tumorigenesis of lung cancer. Furthermore, we found CAB39 played a decisive role in GLUT1 translocation to the plasma membrane and glucose uptake. Our findings provide new evidence to support the critical role of CAB39 in the pathogenesis of HPV-related

lung cancer, and suggest novel therapeutic targets.

ORCID iD

Guang-Ping Wu https://orcid.org/0000-0003 -3478-6868

Statement of human and animal rights

This article does not contain any studies with human or animal subjects.

Supplemental material

Supplemental material for this article is available online.

References

1. Guo H, Nan Y, Zhen Y, *et al.* miRNA-451 inhibits glioma cell proliferation and invasion by downregulating glucose transporter 1. *Tumour Biol* 2016; 37: 13751–13761.

2. Sun H and Jiang P. MicroRNA-451a acts as tumor suppressor in cutaneous basal cell carcinoma. *Mol Genet Genomic Med* 2018; 6: 1001–1009.

3. Liu X, Zhang X, Xiang J, *et al.* miR-451: potential role as tumor suppressor of human hepatoma cell growth and invasion. *Int J Oncol* 2014; 45: 739–745.

4. Li HY, Zhang Y, Cai JH, *et al.* MicroRNA-451 inhibits growth of human colorectal carcinoma cells via downregulation of Pi3k/Akt pathway. *Asian Pac J Cancer Prev* 2013; 14: 3631–3634.

5. Liu Y, Li H, Li LH, *et al.* Mir-451 inhibits proliferation and migration of non-small cell lung cancer cells via targeting LKB1/AMPK. *Eur Rev Med Pharmacol Sci* 2019; 23: 274–280.

6. Khordadmehr M, Jigari-Asl F, Ezzati H, *et al.* A comprehensive review on miR-451: a promising cancer biomarker with therapeutic potential. *J Cell Physiol* 2019; 234: 21716–21731.

7. Goto A, Tanaka M, Yoshida M, *et al.* The low expression of miR-451 predicts a worse prognosis in non-small cell lung cancer cases. *PLoS One* 2017; 12: e0181270.

8. Godlewski J, Nowicki MO, Bronisz A, *et al.* MicroRNA-451 regulates LKB1/AMPK signaling and allows adaptation to metabolic stress in glioma cells. *Mol Cell* 2010; 37: 620–632.

9. Tian Y, Nan Y, Han L, *et al.* MicroRNA miR-451 downregulates the PI3K/AKT pathway through CAB39 in human glioma. *Int J Oncol* 2012; 40: 1105–1112.

10. Jiang L, Yan Q, Fang S, *et al.* Calcium-binding protein 39 promotes hepatocellular carcinoma growth and metastasis by activating extracellular signal-regulated kinase signaling pathway. *Hepatology* 2017; 66: 1529–1545.

11. Koh YW, Lee SJ and Park SY. Differential expression and prognostic significance of GLUT1 according to histologic type of non-small-cell lung cancer and its association with volume-dependent parameters. *Lung Cancer* 2017; 104: 31–37.

12. Roy S, Leidal AM, Ye J, *et al.* Autophagy-dependent shuttling of TBC1D5 controls plasma membrane translocation of GLUT1 and glucose uptake. *Mol Cell* 2017; 67: 84–95.e5.

13. Calado SM, Alves LS, Simão S, *et al.* GLUT1 activity contributes to the impairment of PEDF secretion by the RPE. *Mol Vis* 2016; 22: 761–770.

14. Syrjanen KJ. Condylomatous changes in neoplastic bronchial epithelium. Report of a case. *Respiration* 1979; 38: 299–304.

15. Zhang E, Feng X, Liu F, *et al.* Roles of PI3K/Akt and c-Jun signaling pathways in human papillomavirus type 16 oncoprotein-induced HIF-1alpha, VEGF, and IL-8 expression and in vitro angiogenesis in non-small cell lung cancer cells. *PLoS One* 2014; 9: e103440.

16. Yang JH, Li XY, Wang X, *et al.* Long-term persistent infection of HPV 16 E6 up-regulate SP1 and hTERT by inhibiting LKB1 in lung cancer cells. *PLoS One* 2017; 12: e0182775.

17. Fan R, Hou WJ, Zhao YJ, *et al.* Overexpression of HPV16 E6/E7 mediated HIF-1α upregulation of GLUT1 expression in lung cancer cells. *Tumour Biol* 2016; 37: 4655–4663.

18. Shao JS, Sun J, Wang S, *et al.* HPV16 E6/E7 upregulates HIF-2α and VEGF by inhibiting LKB1 in lung cancer cells. *Tumour Biol* 2017; 39: 1010428317717137.

19. Fu QF, Liu Y, Fan Y, *et al.* Alpha-enolase promotes cell glycolysis, growth, migration, and invasion in non-small cell lung cancer through FAK-mediated PI3K/AKT pathway. *J Hematol Oncol* 2015; 8: 22.

20. Zhuang X, Chen Y, Wu Z, *et al.* Mitochondrial miR-181a-5p promotes glucose metabolism reprogramming in liver cancer by regulating the electron transport chain. *Carcinogenesis* 2019; 41: 972–983.

21. Wang K, Chen M and Wu W. Analysis of microRNA (miRNA) expression profiles reveals 11 key biomarkers associated with non-small cell lung cancer. *World J Surg Oncol* 2017; 15: 175.

22. Warburg O. On the origin of cancer cells. *Science* 1956; 123: 309–314.

23. Deng D, Sun P, Yan C, *et al.* Molecular basis of ligand recognition and transport by glucose transporters. *Nature* 2015; 526: 391–396.

24. Barnes K, Ingram JC, Porras OH, *et al.* Activation of GLUT1 by metabolic and osmotic stress: potential involvement of AMP-activated protein kinase (AMPK). *J Cell Sci* 2002; 115: 2433–2442.

25. Egert S, Nguyen N and Schwaiger M. Myocardial glucose transporter GLUT1: translocation induced by insulin and ischemia. *J Mol Cell Cardiol* 1999; 31: 1337–1344.

26. Lee EE, Ma J, Sacharidou A, *et al.* A protein kinase c phosphorylation motif in GLUT1 affects glucose transport and is mutated in GLUT1 deficiency syndrome. *Mol Cell* 2015; 58: 845–853.

27. Phadngam S, Castiglioni A, Ferraresi A, *et al.* PTEN dephosphorylates AKT to prevent the expression of GLUT1 on plasmamembrane and to limit glucose consumption in cancer cells. *Oncotarget* 2016; 7: 84999–85020.

28. Gwak H, Haegeman G, Tsang BK, *et al.* Cancer-specific interruption of glucose metabolism by resveratrol is mediated through inhibition of Akt/GLUT1 axis in ovarian cancer cells. *Mol Carcinog* 2015; 54: 1529–1540.

29. Wong KY, Liu J and Chan KW. KIF7 attenuates prostate tumor growth through LKB1-mediated AKT inhibition. *Oncotarget* 2017; 8: 54558–54571.

30. Zhang W, Yin L, Song G, *et al.* LKB1 loss cooperating with BRAF V600E promotes melanoma cell invasion and migration by up-regulation MMP-2 via PI3K/Akt/mTOR pathway. *Oncotarget* 2017; 8: 113847–113857.

31. Liemburg-Apers DC, Wagenaars JA, Smeitink JA, *et al.* Acute stimulation of glucose influx upon mitoenergetic dysfunction requires LKB1, AMPK, Sirt2 and mTOR-RAPTOR. *J Cell Sci* 2016; 129: 4411–4423.

32. Zhang Y, Lee S and Xu W. Miltefosine suppression of Pten null T-ALL leukemia via β-catenin degradation through inhibition of pT308-Akt and TGFβ1/Smad3. *Biochem Biophys Res Commun* 2020; 524: 1018–1024.

Visit SAGE journals online
journals.sagepub.com/home/taj

§SAGE journals